Dual specificity phosphatase 22 suppresses mesangial cell hyperproliferation, fibrosis, inflammation and the MAPK signaling pathway in diabetic nephropathy

NA REN[1*], SHANSHAN SHI[2*], NA ZHAO[1] and LINGYAN ZHANG[2]

[1]Department of Endocrinology, First Affiliated Hospital, Heilongjiang University of Chinese Medicine; [2]General Medical Ward, Harbin Institute of Technology Hospital, Harbin, Heilongjiang 150000, P.R. China

Received April 2, 2022; Accepted July 12, 2022

DOI: 10.3892/etm.2022.11680

Abstract. Dual specificity phosphatase 22 (DUSP22) regulates fibrosis and inflammation, which may be implicated in the development of diabetic nephropathy (DN). Hence, the current study aimed to assess the effect of DUSP22 on cell proliferation, apoptosis, fibrosis and inflammation in mouse mesangial cell line (SV40-MES13) under both high glucose (HG) and low glucose (LG) conditions. SV40-MES13 cells were treated with HG and LG, then HG-group cells were transfected with DUSP22 overexpression and control plasmids, meanwhile LG-group cells were transfected with DUSP22 and control siRNAs. Then, cell proliferation using Cell Counting Kit-8, cell apoptosis by TUNEL assay, protein expression using western blotting, inflammatory cytokines using ELISA and RNA using reverse transcription-quantitative PCR were determined. DUSP22 mRNA and protein were decreased in SV40-MES13 cells under the HG condition compared with those under the LG condition. Under the HG condition, DUSP22 overexpression suppressed SV40-MES13 cell proliferation at 48 and 72 h as well as Bcl2, but it facilitated TUNEL-reflected apoptotic rate and cleaved-caspase-3; besides, DUSP22 overexpression restrained proteins of fibronectin 1, collagen I, transforming growth factor beta 1, and their corresponding mRNAs. As to the inflammation, DUSP22 overexpression downregulated TNF-α, IL-1β, IL-6 and IL-12 under the HG condition. By contrast, DUSP22 siRNA promoted SV40-MES13 cell proliferation, fibrosis and inflammation, but attenuated apoptosis in SV40-MES13 cells under the LG condition. Additionally, DUSP22 overexpression inactivated phosphorylated (p)-ERK, p-JNK, and p-P38 in HG-treated SV40-MES13 cells; differently, DUSP22 small interfering RNA facilitated them under the LG condition. In conclusion, DUSP22 suppresses HG-induced mesangial cell hyperproliferation, fibrosis, inflammation and the MAPK pathway, implying its potency in DN treatment.

Correspondence to: Professor Lingyan Zhang, General Medical Ward, Harbin Institute of Technology Hospital, 2 Xiaowai Street, Nangang, Harbin, Heilongjiang 150000, P.R. China
E-mail: yalan8003858384@163.com

*Contributed equally

Key words: dual specificity phosphatase 22, diabetic nephropathy, fibrosis, inflammation, MAPK signaling pathway

Introduction

Diabetic nephropathy (DN), clinically manifested as persistent albuminuria and glomerular filtration rate decrement, is a common complication of diabetes; in detail, DN prevalence in diabetes patients ranges from 18.7-24.0% in China (1-3). At present, the management of DN mainly contains blood glucose/pressure control and lipid control (4,5). Nevertheless, DN remains the leading reason for end-stage kidney disease; among which irreversible fibrosis, excessive proliferation and inflammation flare in renal glomerular basement membrane cells and mesangial cells are the main pathological manifestations during the progression of DN (6-8). Hence, exploring the underlying mechanism of these pathological alterations may help improve DN management more effectively.

Dual specificity phosphatase (DUSP) 22, also known as Jun N-terminal kinase pathway-associated phosphatase, is a tyrosine-specific protein participating in several cellular processes (including cell proliferation and apoptosis) due to its unique function of dephosphorylating serine/threonine (9-11). For instance, a previous study revealed that DUSP22-knockdown T cells accelerate dysregulation of inflammatory cytokines (11). Another study found that DUSP22 regulates the transcription of interleukin (IL)-6 and inflammation response via dephosphorylating signal transducer and activator of transcription 3 (STAT3) (10). Meanwhile, DUSP22 is an important regulator of the mitogen-activated protein kinases (MAPKs), while the activation of MAPKs mediates mesangial cell apoptosis and tubulointerstitial fibrosis (12,13). Combining that inflammation and glomerular fibrosis are implicated in DN pathogenesis, it was hypothesized that DUSP22 may serve as a protective factor of DN, while it has not been studied yet.

Hence, the current study aimed to assess the effect of DUSP22 on cell proliferation, apoptosis, fibrosis, inflammation

and its potential mediated signaling pathway in mouse mesangial cell line (SV40-MES13) under both high glucose (HG) and low glucose (LG) conditions.

Materials and methods

Cell culture. Considering that the SV40-MES13 cells were commonly used to establish the cellular DN model according to previous studies, the same cell line was chosen in the present study (14-17). SV40-MES13 was obtained from National Collection of Authenticated Cell Cultures (Shanghai, China). Cells were maintained in DMEM/F12 medium (HyClone; Cytiva) supplemented with 5% fetal bovine serum (Merck KGaA) and 1% penicillin/streptomycin (Beyotime Institute of Biotechnology) at 37˚C and 5% CO_2.

Cell transfection. DUSP22 overexpression and control plasmids were purchased from Sangon Biotech Co., Ltd. DUSP22 and control small interfering (si) RNAs were synthesized by Shanghai GenePharma Co., Ltd. Briefly, SV40-MES13 cells were seeded in six-well ($2x10^5$ cells/well) or 96-well plate ($5x10^3$ cells/well) and cultured into 80% confluence. Cells were then transfected (100 or 5 pM) into cells using HilyMAX Reagent (Invitrogen; Thermo Fisher Scientific, Inc.) at 37˚C for 6 h according to the manufacturers' protocol. The sense sequences of siRNAs were as follows: DUSP22, 5'-CGGGCC TGTACATTGGCAACTTCAA-3'; and control, 5'-CGGGTC CATTTACGGCAATTGCCAA-3'.

Glucose treatment. The SV40-MES13 cells were seeded in six-well plates ($2x10^5$ cells/well) and divided into HG and LG groups. In the HG group, SV40-MES13 cells were stimulated with 25 mM D-glucose (Shanghai Aladdin Biochemical Technology Co., Ltd.) for 48 h to establish cellular DN model (14-18), and transfected with DUSP22 overexpression plasmid (HG-oe-DUSP22) or control plasmid (HG-oe-NC) as aforementioned. In the LG group, SV40-MES13 cells were stimulated with 5.5 mM D-glucose supplemented with 19.5 mM D-mannitol (Sigma-Aldrich; Merck KGaA) for 48 h, and transfected with DUSP22 siRNA (LG-si-DUSP22) or siRNA control (LG-si-NC) as aforementioned. Untransfected cells cultured in HG or LG medium were used as control group (HG-Control or LG-Control). Cells were then incubated for 48 h, and harvested for reverse transcription-quantitative PCR (RT-qPCR), cell apoptosis and western blotting assays. The cell supernatant was used for inflammatory cytokines assessment using ELISA.

Cell proliferation assay. Cell proliferation detection of SV40-MES13 cells was performed using Cell Counting Kit-8 (CCK-8; Dojindo Laboratories, Inc.). In brief, cells in the HG or LG group were plated on a 96-well plate ($5x10^3$ cells/well) and transfected as indicated. At 0, 24, 48 and 72 h after transfection, 10 μl CCK-8 detection buffer was added and cells were incubated for 2 h at 37˚C. A microplate reader (Tosoh Corporation) was adopted to assess cell proliferation with an optical density (OD) value of 450 nm being measured.

Cell apoptosis assay. The TUNEL detection kit (Elabscience Biotechnology, Inc.) was used for assessing cell apoptotic rate after treatment. In brief, SV40-MES13 cells were fixed with 4% paraformaldehyde (Wuhan Servicebio Technology Co., Ltd.) for 15 min and incubated with Triton X-100 (Wuhan Servicebio Technology Co., Ltd.) for 10 min at 37˚C. Afterwards, cells were incubated with apoptosis detection buffer for 0.5 h at 37˚C. After being stained with DAPI (5 mg/l; Sangon Biotech Co., Ltd.) for 10 min and sealed by Antifade Mounting Medium (Beyotime Institute of Biotechnology), cell apoptotic rate was evaluated using fluorescence microscope (Olympus Corporation) with five random fields being selected.

ELISA. The supernatant of SV40-MES13 cells was collected at 48 h after treatment. The content of inflammatory cytokines in cell supernatant was detected using mouse tumor necrosis factor-alpha (TNF-α; cat. no. D721150), IL-1β (cat. no. D721017), IL-6 (cat. no. D721022), and IL-12 (cat. no. D721174) ELISA kits (Sangon Biotech Co., Ltd.), respectively. The experiment was performed in accordance with the manufacturer's protocol. The OD value at 450 nm was measured using a microplate reader (Tosoh Corporation).

RNA extraction and RT-qPCR. Total RNA of SV40-MES13 cells was extracted using RNAzol® RT (Sigma-Aldrich; Merck KGaA). The concentration of RNA was analyzed using Qubit-4 Flurometer (Invitrogen; Thermo fisher Scientific, Inc.). Reverse Transcription kit (Qiagen GmbH) was used for cDNA synthesis in accordance with the kit's protocol. The quantification of DUSP22, fibronectin 1 (FN1), collagen I (COL1A1) and transforming growth factor beta 1 (TGF-β1) was performed using the SYBR Green PCR kit (Qiagen GmbH) and normalized to the level of β-actin. The thermocycling conditions of qPCR were as follows: 95˚C for 5 min, 1 cycle; 95˚C for 10 sec, 61˚C for 30 sec, 40 cycles. The results were calculated using the $2^{-\Delta\Delta Cq}$ method (19). The sequences of primers used for RT-qPCR were as follows: DUSP22 forward, 5'-GCC AGGCCTATGTTGGAGGGAGTT-3' and reverse, 5'-TGT ATGCGATCACCAGTGTCAC-3'; FN1 forward, 5'-ATGTGG ACCCCTCCTGATAGT and reverse, 5'-GCCCAGTGATTT CAGCAAAGG-3'; COL1A1 forward, 5'-CTCGTGGATTGC CTGGAACA-3' and reverse, 5'-GCACCAACAGCACCATCG T-3'; TGF-β1 forward, 5'-TGACGTCACTGGAGTTGTACG G-3' and reverse, 5'-GGTTCATGTCATGGATGGTGC-3'; and β-actin forward, 5'-AAGACCTCTATGCCAACACAGTG-3' and reverse, 5'-CATCGTACTCCTGCTTGCTGAT-3'.

Western blot analysis. SV40-MES13 cells were lysed in RIPA containing 1% protease and phosphatase inhibitor cocktail (cat. No. P1048; Beyotime Institute of Biotechnology) for protein extraction. The protein quantification was performed using the BCA quantification kit (Beyotime Institute of Biotechnology). A total of 30 μg protein of each group were separated by 4-20% SDS-PAGE precast gels and transferred into polyvinylidene difluoride membrane (both from Beyotime Institute of Biotechnology). The membrane was then blocked using 5% BSA solution for 1.5 h at 37˚C and incubated overnight at 4˚C with the following primary antibodies: DUSP22 (1:2,000; cat. no. ab70124), caspase 3 (1:5,000; cat. no. ab184787), cleaved caspase 3 (1:1,000; cat. no. ab214430; all from Abcam), Bcl2 (1:2,000; cat. no. AF6139), FN1 (1:1,000; cat. no. AF5335), COL1A1

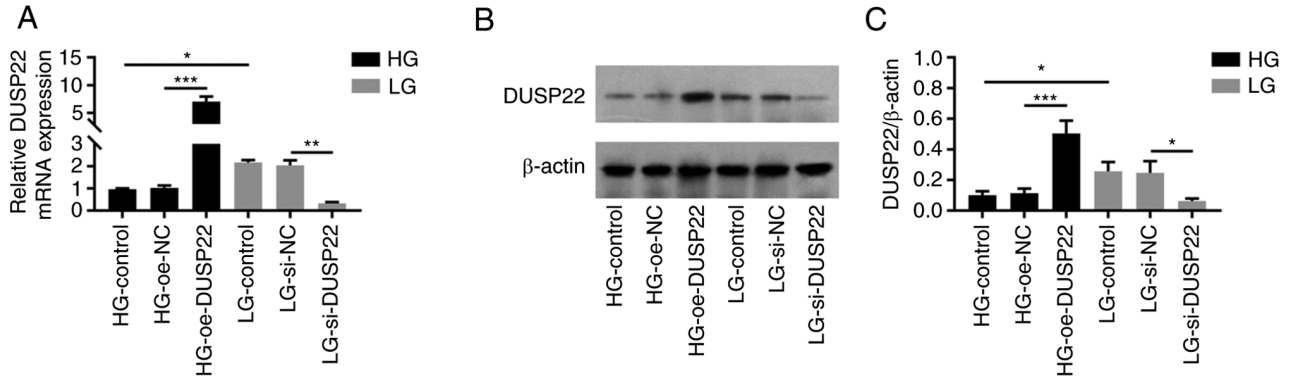

Figure 1. DUSP22 expression after transfection in SV40-MES13 cells. (A) DUSP22 mRNA expression among groups. (B) Western blot analysis exhibiting DUSP22 protein expression among groups. (C) Densitometric analysis of western blotting at panel B. *P<0.05, **P<0.01 and ***P<0.001. DUSP22, dual specificity phosphatase 22; HG, high glucose; LG, low glucose; oe, overexpression; si-, small interfering; NC, negative control.

(1:1,000; cat. no. AF7001; all from Affinity Biosciences, Ltd.), TGF-β1 (1:2,000; cat. no. ab215715; Abcam), p-extracellular signal-regulated kinase (ERK) (Thr202/Tyr204) (1:1,000; cat. no. AF1015), ERK (1:1,000; cat. no. AF0155), p-c-Jun N-terminal kinase (JNK) (Tyr185) (1:2,000; cat. no. AF3318; all from Affinity Biosciences, Ltd.), JNK (1:1,000; cat. no. GB114321; Wuhan Servicebio Technology Co., Ltd.), p-P38 (Thr180/Tyr182) (1:1,000; cat. no. AF4001), P38 (1:1,000; cat. no. AF6456), Ki-67 (1:1,500; cat. no. AF0198; all from Affinity Biosciences, Ltd.) and β-actin (1:5,000; cat. no. GB15003; Wuhan Servicebio Technology Co., Ltd.). Afterwards, the membranes were incubated with HRP-conjugated goat anti-rabbit secondary antibodies (1:10,000; cat. no. ab205718; Abcam) for 1 h at 37˚C. Finally, ECL Plus kit (Shanghai Yeasen Biotechnology Co., Ltd.) was used for chemiluminescence. Considering the similar molecular weights of caspase 3, cleaved caspase 3, Bcl2, and β-actin, the membrane was stripped and re-probed for the second antibody once the first protein band was visualized (20). The densitometric analysis was performed using Image J 1.8 (National Institutes of Health).

Statistical analysis. GraphPad 7.0 software (GraphPad Software, Inc.) was used for data analysis and graph plotting. Multigroup comparison was analyzed by one-way ANOVA followed by Tukey's post hoc test. The data are presented as the mean value ± standard deviation, and each experiment was replicated for three times. P<0.05 was considered to indicate a statistically significant difference.

Results

DUSP22 expression in SV40-MES13 cells. DUSP22 mRNA expression was decreased in HG-Control group compared with LG-Control group (P<0.05); moreover, DUSP22 expression was increased in HG-oe-DUSP22 group compared with that in HG-oe-NC group (P<0.001), but it was decreased in the LG-si-DUSP22 group compared with the LG-si-NC group (P<0.01; Fig. 1A), which indicated that the transfection was successful. Furthermore, DUSP22 protein expression showed a similar trend to DUSP22 mRNA expression among groups (all P<0.05; Fig. 1B and C).

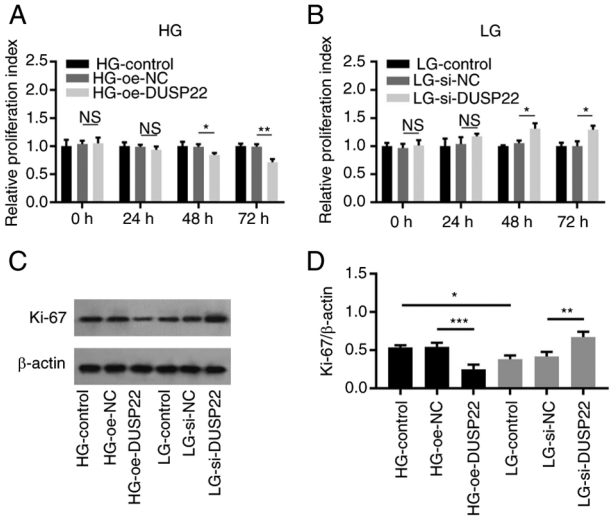

Figure 2. DUSP22 suppresses SV40-MES13 cell proliferation. (A and B) Effect of DUSP22 on SV40-MES13 cell proliferation under the (A) HG and (B) LG conditions. (C) Western blot analysis demonstrating the effect of DUSP22 on Ki-67 in SV40-MES13 cells. (D) Densitometric analysis of western blotting at panel C. *P<0.05, **P<0.01 and ***P<0.001. DUSP22, dual specificity phosphatase 22; HG, high glucose; LG, low glucose; oe, overexpression; si-, small interfering; NC, negative control; ns, no significance.

Effect of DUSP22 on SV40-MES13 cell proliferation. Cell proliferation at 48 (P<0.05) and 72 h (P<0.01) was reduced in the HG-oe-DUSP22 group compared with that in the HG-oe-NC group (Fig. 2A). On the contrary, cell proliferation at 48 (P<0.05) and 72 h (P<0.05) was elevated in the LG-si-DUSP22 group compared with the LG-si-NC group (Fig. 2B). Additionally, the proliferation biomarker Ki-67 was determined to further validate the results, which showed that Ki-67 was decreased in the HG-oe-DUSP22 group compared with the HG-oe-NC group (P<0.001); while it was increased in the LG-si-DUSP22 group compared with that in the LG-si-NC group (P<0.01; Fig. 2C and D).

Effect of DUSP22 on SV40-MES13 cell apoptosis. TUNEL-reflected apoptotic rate (P<0.001; Fig. 3A and B) and the expression of cleaved caspase 3 (P<0.01; Fig. 3C and D) were

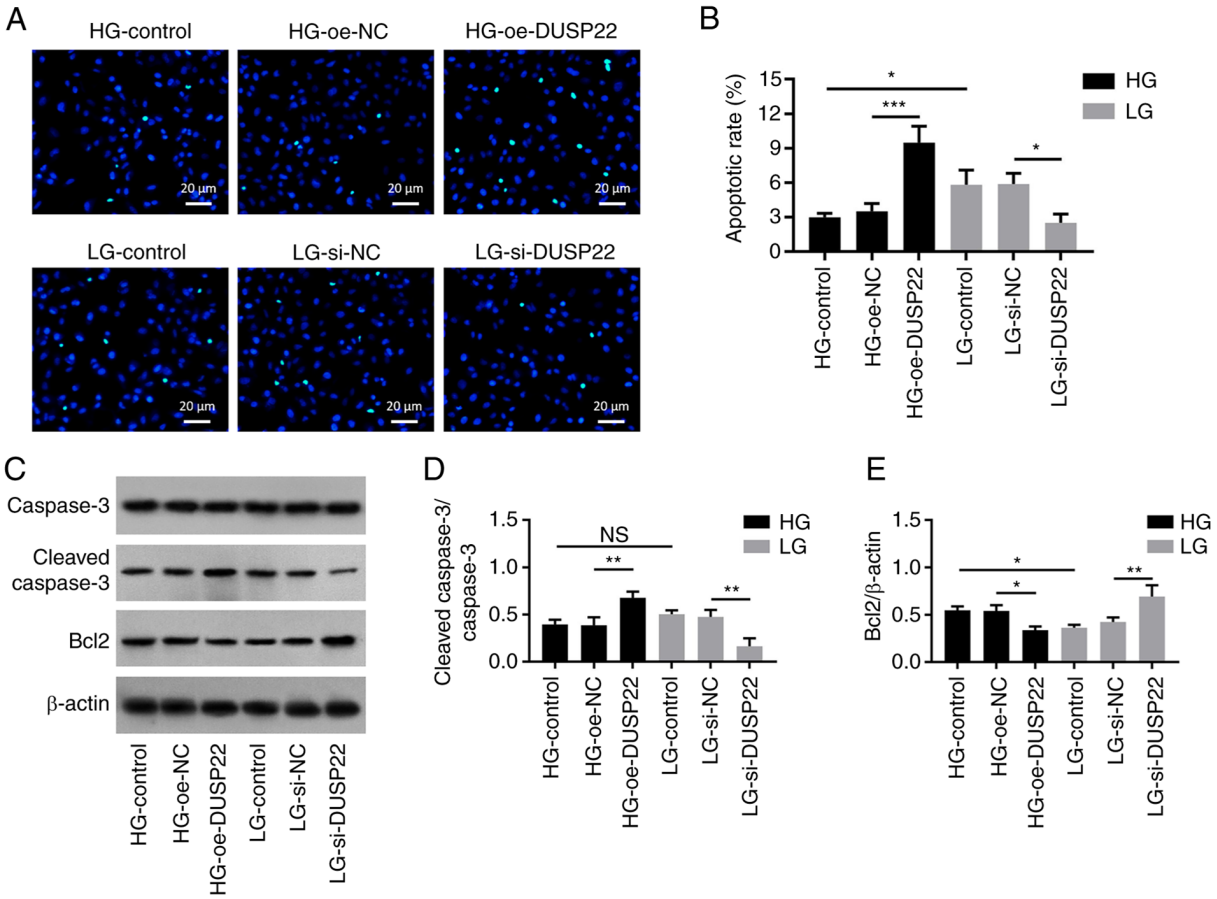

Figure 3. DUSP22 facilitates SV40-MES13 cell apoptosis. (A) Example images of TUNEL staining. (B) Apoptotic rate among groups. (C) Western blot analysis revealing the effect of DUSP22 on (C and D) cleaved caspase 3 and (C and E) Bcl2 expression levels in SV40-MES13 cells. (D and E) Densitometric analysis of western blotting at panel C. *P<0.05, **P<0.01 and ***P<0.001. DUSP22, dual specificity phosphatase 22; HG, high glucose; LG, low glucose; oe, overexpression; si-, small interfering; NC, negative control; ns, no significance.

elevated, while the expression of Bcl2 (P<0.05; Fig. 3C and E) was reduced in the HG-oe-DUSP22 group compared with those in the HG-oe-NC group. By contrast, TUNEL-reflected apoptotic rate (P<0.05) and expression of cleaved caspase 3 (P<0.01) were decreased, but expression of Bcl2 (P<0.01) was increased in the LG-si-DUSP22 group compared with the LG-si-NC group.

Effect of DUSP22 on SV40-MES13 cell fibrosis. FN1 mRNA (P<0.05; Fig. 4A), COL1A1 mRNA (P<0.01; Fig. 4B) and TGF-β1 mRNA (P<0.001; Fig. 4C) levels were reduced in the HG-oe-DUSP22 group compared with the HG-oe-NC group; while they were upregulated in the LG-si-DUSP22 group compared with the LG-si-NC group (all P<0.01). In terms of fibrosis-related proteins (Fig. 4D), FN1 protein (Fig. 4E), COL1A1 I protein (Fig. 4F) and TGF-β1 protein (Fig. 4G) displayed a similar trend among groups with their corresponding mRNAs (all P<0.05).

Effect of DUSP22 on SV40-MES13 cell inflammation. TNF-α (P<0.05; Fig. 5A), IL-6 (P<0.05; Fig. 5B), IL-1β (P<0.01; Fig. 5C) and IL-12 (P<0.05; Fig. 5D) were downregulated in the HG-oe-DUSP22 group compared with those in the HG-oe-NC group; while TNF-α (P<0.05), IL-6 (P<0.05), and IL-1β (P<0.01) were significantly increased in the LG-si-DUSP22 group compared with the LG-si-NC, except for IL-12 (P>0.05).

Determination of DUSP22 mediated pathways. As revealed using western blot analysis (Fig. 6A), p-ERK (P<0.001), p-JNK (P<0.05) and p-P38 (P<0.01) expression levels were decreased in the HG-oe-DUSP22 group compared with the HG-oe-NC group; by contrast, they were increased in the LG-si-DUSP22 group compared with the LG-si-NC group (all P<0.05; Fig. 6B).

Discussion

DUSPs are widely known as dephosphorylated proteins which serve as protective factors in inflammation-related injuries via inactivating the MAPK signaling pathway (21-23). For example, a recent study revealed that DUSP26 knockdown promotes fibrosis in kidney glomeruli via enhancing TGF-β1 expression, then renal injury and dysfunction of DN are greatly accelerated (22). As a member of the DUSP family, DUSP22 shares a similar function of regulating MAPK signaling, which is a crucial pathway in the development of renal diseases (24,25). For instance, a recent study identified the dysregulation of DUSP22 in IgA nephropathy (26). In addition, it was demonstrated that the aberrant DUSP22 expression is

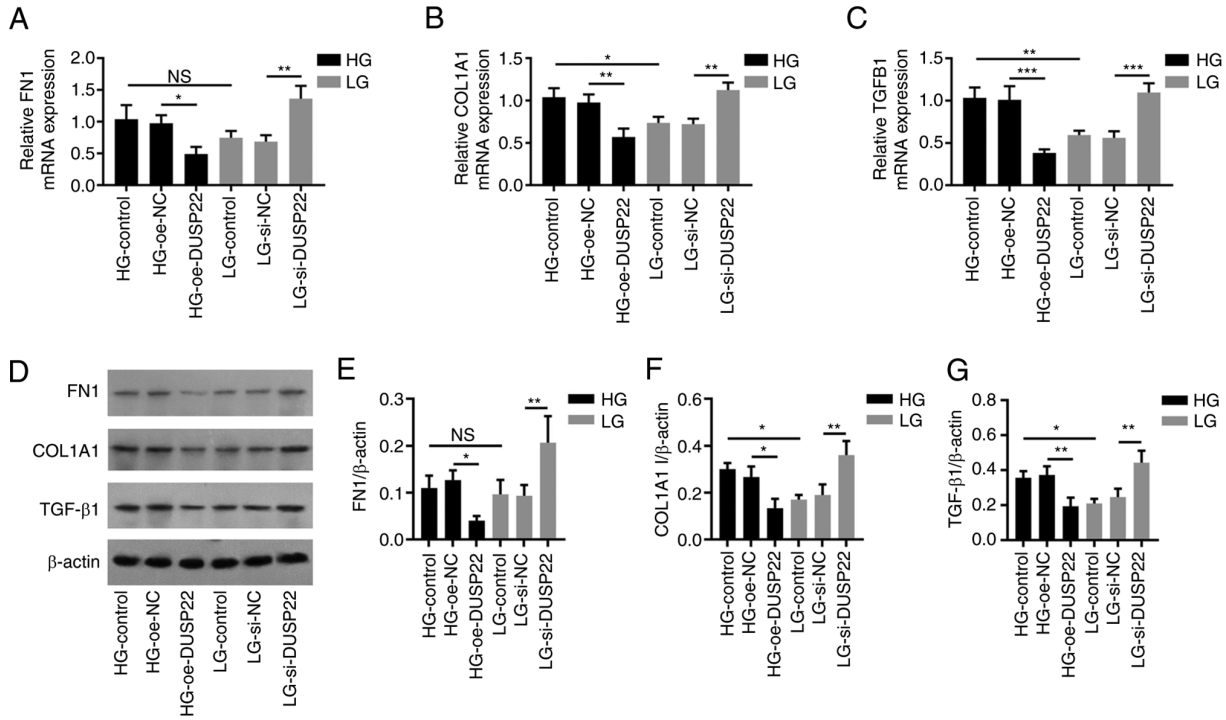

Figure 4. DUSP22 suppresses SV40-MES13 cell fibrosis. (A-C) Effect of DUSP22 on mRNA levels of (A) FN1, (B) COL1A1, and (C) TGF-β1 in SV40-MES13 cells. (D) Western blot analysis revealing the effect of DUSP22 on (D and E) FN1, (D and F) COL1A1 and (D and G) TGF-β1 in SV40-MES13 cells. (E-G) Densitometric analysis of western blotting at panel D. *P<0.05, **P<0.01 and ***P<0.001. DUSP22, dual specificity phosphatase 22; FN1, fibronectin 1; COL1A1, collagen I; TGF-β1, transforming growth factor beta 1; HG, high glucose; LG, low glucose; oe, overexpression; si-, small interfering; NC, negative control; ns, no significance.

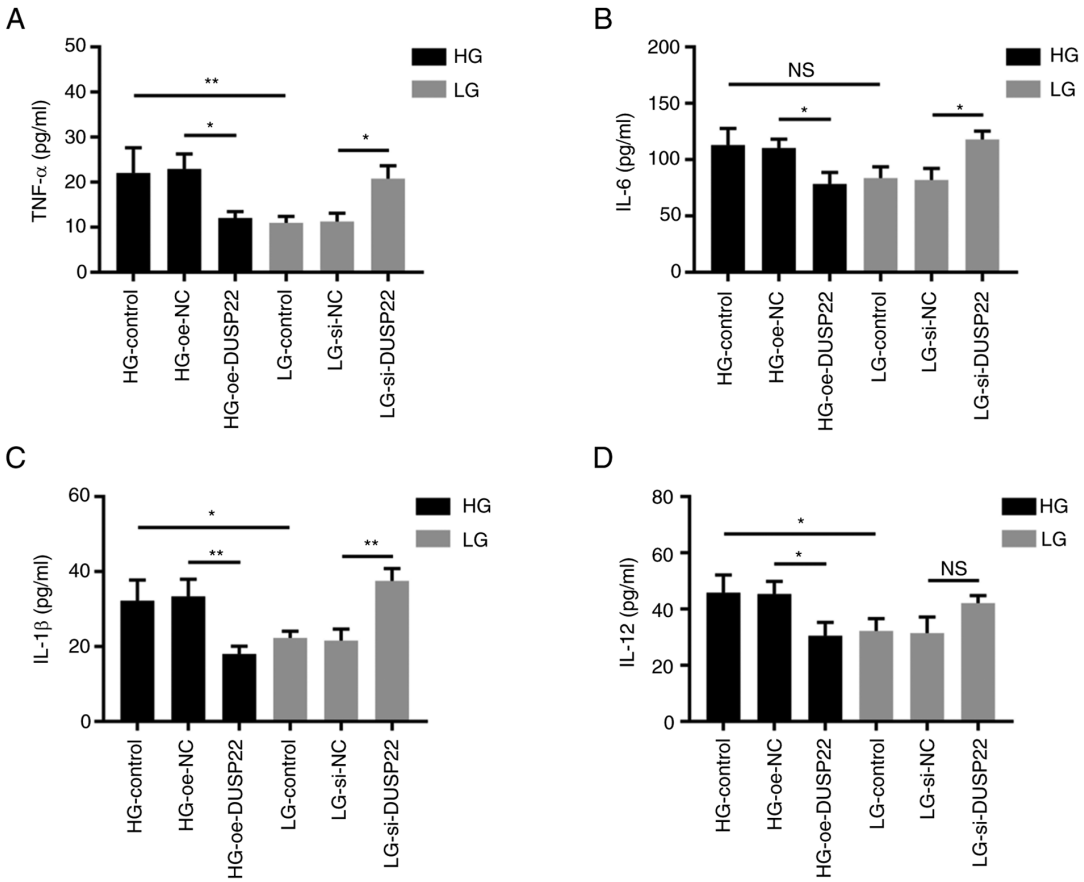

Figure 5. DUSP22 suppresses inflammation in SV40-MES13 cells. (A-D) Effect of DUSP22 on (A) TNF-α, (B) IL-6, (C) IL-1β and (D) IL-12 in SV40-MES13 cells. *P<0.05 and **P<0.01. DUSP22, dual specificity phosphatase 22; HG, high glucose; LG, low glucose; oe, overexpression; si-, small interfering; NC, negative control.

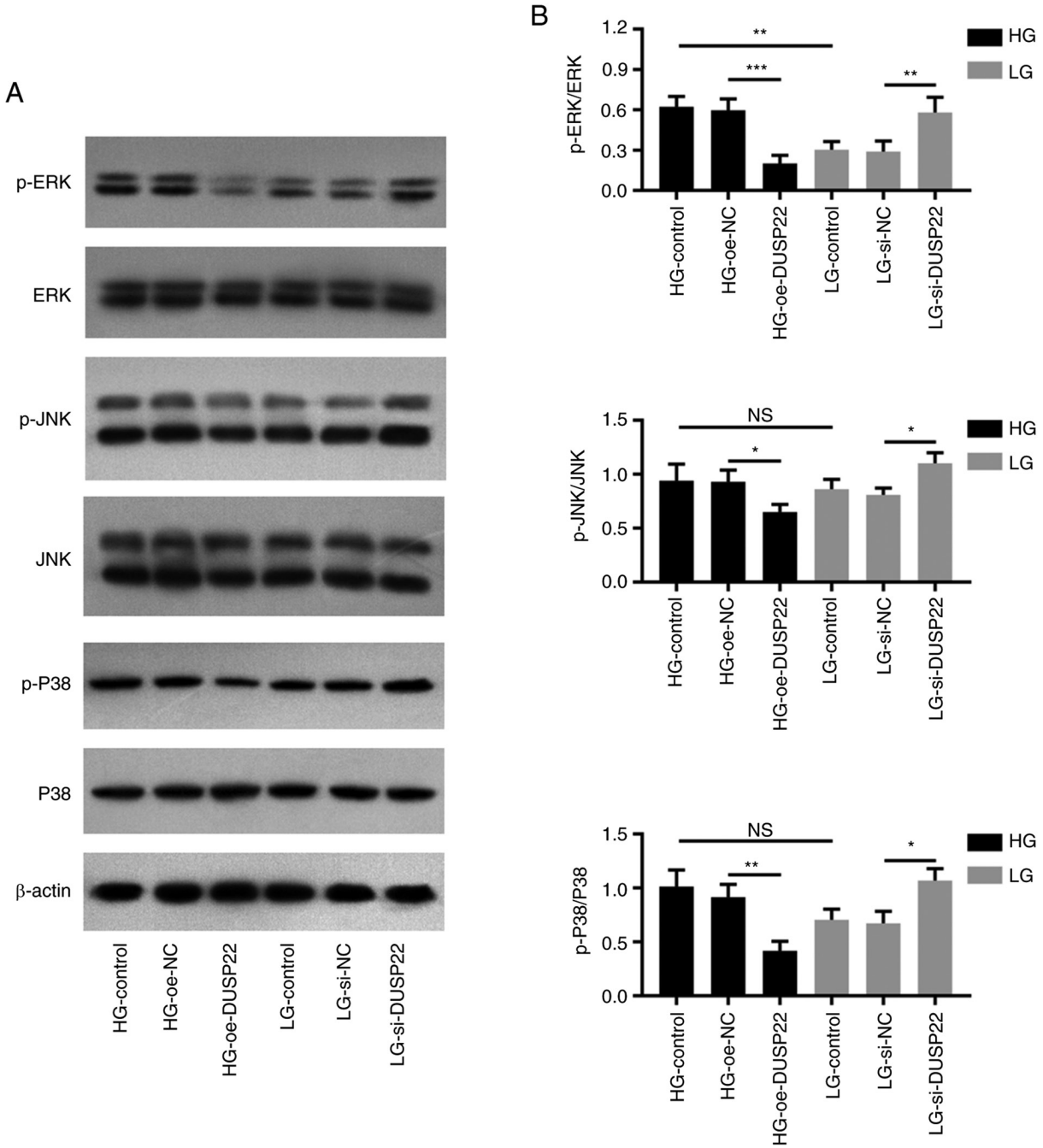

Figure 6. DUSP22 suppresses the MAPK signaling pathway in diabetic nephropathy. (A) Western blot analysis demonstrating the effect of DUSP22 on the MAPK signaling pathway in SV40-MES13 cells. Densitometric analysis of western blotting at panel A revealing the effect of DUSP22 on p-ERK, p-JNK and p-P38 in SV40-MES13 cells. (B) Impact of DUSP22 on p-ERK, p-JNK, and p-P38 in SV40-MES13 cells. *P<0.05, **P<0.01 and ***P<0.001. DUSP22, dual specificity phosphatase 22; p-, phosphorylated; HG, high glucose; LG, low glucose; oe, overexpression; si-, small interfering; NC, negative control; ns, no significance.

linked with increased disease activity and poor renal outcomes in patients with systemic lupus erythematosus nephritis (27). The involvement of DUSP22 in DN pathogenesis remains unclear; thus, the present study was conducted and it was found that DUSP22 overexpression promoted mesangial cell apoptosis, but it suppressed mesangial cell proliferation and fibrosis under the HG condition; while DUSP22 siRNA caused the opposite effect in LG-treated mesangial cells. These findings suggested that DUSP22 weakened DN hyperproliferation and fibrosis, which may be due to the following possible reasons: i) DUSP22 overexpression restrained MAPKs (including ERK, JNK, and p38), while both JNK and p38 may enhance renal cell proliferation but inhibit renal cell apoptosis via reducing anti-apoptotic proteins (such as Bcl2) (28,29). Therefore, DUSP22 in SV40-MES13 cells inhibited cell proliferation but promoted cell apoptosis; ii) DUSP22 suppressed epithelial-to-mesenchymal transition (EMT) via restraining the p38/MAPK pathway; meanwhile, EMT could accelerate HG-induced renal fibrosis (23,30,31). Thus, DUSP22 reduced renal fibrosis in SV40-MES13 cells. Furthermore, the results of the TUNEL assay and cleaved-caspase-3 shared a similar trend. The only discrepancy was that the apoptotic rate

was decreased, while cleaved caspase 3 only demonstrated a decreasing trend (lacked statistical significance) in the HG-Control group compared with the LG-Control group. A possible explanation may be that cleaved caspase 3 protein expression and TUNEL-reflected cell apoptosis themselves presented a mild difference (32,33).

In line with other chronic renal diseases, inflammation dominates in the development of DN; in turn, the HG environment can induce inflammatory injury as well (34). Accordingly, it was observed in the current study that TNF-α, IL-1β and IL-12 were elevated in mesangial cells under the HG condition compared with those under the LG condition. With regard to the effect of DUSP22 on inflammation, it has been recognized that DUSP22 attenuates inflammatory cytokine recruitment via inhibiting several signaling pathways [such as the T cell receptor (TCR)] signaling pathway and the nuclear factor-kappa B pathway] (11,27,35). For instance, a previous study revealed that IL-17, IL-6 and interferon-γ are increased in DUSP22-knockout $CD4^+$ T cells through the modulation of TCR signaling (11). Similarly, it was identified in the present study that DUSP22 overexpression downregulated TNF-α, IL-6, IL-1β and IL-12 in HG-treated SV40-MES13 cells; while DUSP22 siRNA showed the opposite effect on them under the LG condition, which indicated that DUSP22 inhibited inflammation in DN. A probable explanation may be the following: DUSP22 could inactive the MAPK pathway while the latter triggered several inflammatory pathways; subsequently, the excessive secretion of pro-inflammatory cytokines (including TNF-α, IL-6, IL-1β and IL-12) was suppressed (35).

Additionally, SV40-MES13 cells in the HG group were stimulated using 25 mM D-glucose for 48 h to establish the cellular DN model and it was found that HG protected from apoptosis. Meanwhile, certain previous studies also identified that HG promotes mesangial cell proliferation and fibrosis at the same concentration (18,36). Whereas one study revealed that HG may increase apoptosis in human renal proximal tubular epithelial cells under 30 mmol/l D-glucose (37), which may be possibly due to that different glucose concentrations and different cells may cause different trends. TGF-β1 was strongly activated in the murine renal mesangial cell line, which induced cell proliferation and fibrosis in high-glucose media (38). On the contrary, the HG condition activated p38 mitogen-activated protein kinase (p38 MAPK) in human renal proximal tubular epithelial cells, which further promoted cell apoptosis (37,39). Hence, different phenomena are observed in different cell types.

The activation of the MAPK signaling pathway (contains ERK, JNK and p38) promotes inflammation response and cell death in renal tubular and membrane (40,41). As to the detailed role of the MAPK signaling pathway in DN pathogenesis, a previous study revealed that the MAPK pathway modulates cell apoptosis, over-production of inflammatory cytokines and extracellular matrix dysregulation of DN (25). In the present study, it was found that DUSP22 overexpression restrained p-JNK, p-ERK and p-p38 under HG-treated SV40-MES13 cells, whereas DUSP22 siRNA exhibited the opposite effect under the LG condition, which suggested that DUSP22 blocked the MAPK signaling pathway in SV40-MES13 cells. The limitations to the present study were non-negligible: Firstly, HG-group cells were only transfected with DUSP22 overexpression plasmid, and LG-group cells were only transfected with DUSP22 siRNA. Therefore, further study transfecting HG-group and LG-group cells with both DUSP22 overexpression and DUSP22 siRNA was necessary. Secondly, the flow cytometry experiments were warranted in further studies to validate the apoptotic results. Thirdly, since no human cells were used in the present study, there exists a potential limitation in translating results into clinical applications. Fourthly, renal mesangial and endothelial cells did not downregulate glucose transporters under HG conditions; subsequently, the Krebs cycle resulted in more nicotinamide adenine dinucleotide (42). In this case, the same cell number was expected to provide a more intense signal in the CCK-8 assay when cultured under HG conditions. Thus, further study should conduct the BrdU assay to verify the cell proliferation results. In conclusion, it was revealed that DUSP22 suppresses HG-induced mesangial cell hyperproliferation, fibrosis, inflammation and the MAPK pathway, indicating its potency in DN treatment.

Acknowledgements

Not applicable.

Funding

No funding was received.

Availability of data and materials

The datasets used and/or analyzed during the current study are available from the corresponding author on reasonable request.

Authors' contributions

NR and SS contributed equally to the conception and design and drafted the manuscript. LZ and NZ contributed to analyzing the data and revised the manuscript critically for important intellectual content. NR and SS confirm the authenticity of all the raw data. All authors read and approved the final manuscript, and agreed to be accountable for all aspects of the work in ensuring that questions related to the accuracy or integrity of any part of the work are appropriately investigated and resolved.

Ethics approval and consent to participate

Not applicable.

Patient consent for publication

Not applicable.

Competing interests

The authors declare that they have no competing interests.

References

1. Samsu N: Diabetic nephropathy: Challenges in pathogenesis, diagnosis, and treatment. Biomed Res Int 2021: 1497449, 2021.
2. Sagoo MK and Gnudi L: Diabetic nephropathy: An overview. Methods Mol Biol 2067: 3-7, 2020.

3. Zhang XX, Kong J and Yun K: Prevalence of diabetic nephropathy among patients with type 2 diabetes Mellitus in China: A meta-analysis of observational studies. J Diabetes Res 2020: 2315607, 2020.
4. Selby NM and Taal MW: An updated overview of diabetic nephropathy: Diagnosis, prognosis, treatment goals and latest guidelines. Diabetes Obes Metab 22 (Suppl 1): S3-S15, 2020.
5. Yamazaki T, Mimura I, Tanaka T and Nangaku M: Treatment of diabetic kidney disease: Current and future. Diabetes Metab J 45: 11-26, 2021.
6. Agarwal R: Pathogenesis of diabetic nephropathy. Chronic kidney disease and type 2 diabetes. Arlington (VA) American Diabetes Association 2021.
7. Cao Z and Cooper ME: Pathogenesis of diabetic nephropathy. J Diabetes Investig 2: 243-247, 2011.
8. Yu SM and Bonventre JV: Acute kidney injury and progression of diabetic kidney disease. Adv Chronic Kidney Dis 25: 166-180, 2018.
9. Chen AJ, Zhou G, Juan T, Colicos SM, Cannon JP, Cabriera-Hansen M, Meyer CF, Jurecic R, Copeland NG, Gilbert DJ, *et al*: The dual specificity JKAP specifically activates the c-Jun N-terminal kinase pathway. J Biol Chem 277: 36592-36601, 2002.
10. Sekine Y, Ikeda O, Hayakawa Y, Tsuji S, Imoto S, Aoki N, Sugiyama K and Matsuda T: DUSP22/LMW-DSP2 regulates estrogen receptor-alpha-mediated signaling through dephosphorylation of Ser-118. Oncogene 26: 6038-6049, 2007.
11. Li JP, Yang CY, Chuang HC, Lan JL, Chen DY, Chen YM, Wang X, Chen AJ, Belmont JW and Tan TH: The phosphatase JKAP/DUSP22 inhibits T-cell receptor signalling and autoimmunity by inactivating Lck. Nat Commun 5: 3618, 2014.
12. Li J, Jin S, Barati MT, Rane S, Lin Q, Tan Y, Cai L and Rane MJ: ERK and p38 MAPK inhibition controls NF-E2 degradation and profibrotic signaling in renal proximal tubule cells. Life Sci 287: 120092, 2021.
13. Grynberg K, Ma FY and Nikolic-Paterson DJ: The JNK signaling pathway in renal fibrosis. Front Physiol 8: 829, 2017.
14. Xiao L, Chen A, Gao Q, Xu B, Guo X and Guan T: Pentosan polysulfate ameliorates fibrosis and inflammation markers in SV40 MES13 cells by suppressing activation of PI3K/AKT pathway via miR-446a-3p. BMC Nephrol 23: 105, 2022.
15. Wu R, Niu Z, Ren G, Ruan L and Sun L: CircSMAD4 alleviates high glucose-induced inflammation, extracellular matrix deposition and apoptosis in mouse glomerulus mesangial cells by relieving miR-377-3p-mediated BMP7 inhibition. Diabetol Metab Syndr 13: 137, 2021.
16. Chen Z, Gao H, Wang L, Ma X, Tian L, Zhao W, Li K, Zhang Y, Ma F, Lu J, *et al*: Farrerol alleviates high glucose-induced renal mesangial cell injury through the ROS/Nox4/ERK1/2 pathway. Chem Biol Interact 316: 108921, 2020.
17. Zhao L, Chen H, Zeng Y, Yang K, Zhang R, Li Z, Yang T and Ruan H: Circular RNA circ_0000712 regulates high glucose-induced apoptosis, inflammation, oxidative stress, and fibrosis in (DN) by targeting the miR-879-5p/SOX6 axis. Endocr J 68: 1155-1164, 2021.
18. Zhang P, Sun Y, Peng R, Chen W, Fu X, Zhang L, Peng H and Zhang Z: Long non-coding RNA Rpph1 promotes inflammation and proliferation of mesangial cells in diabetic nephropathy via an interaction with Gal-3. Cell Death Dis 10: 526, 2019.
19. Livak KJ and Schmittgen TD: Analysis of relative gene expression data using real-time quantitative PCR and the 2(-Delta Delta C(T)) Method. Methods 25: 402-408, 2001.
20. Aggarwal M, Saxena R, Asif N, Sinclair E, Tan J, Cruz I, Berry D, Kallakury B, Pham Q, Wang TTY and Chung FL: p53 mutant-type in human prostate cancer cells determines the sensitivity to phenethyl isothiocyanate induced growth inhibition. J Exp Clin Cancer Res 38: 307, 2019.
21. Huang CY and Tan TH: DUSPs, to MAP kinases and beyond. Cell Biosci 2: 24, 2012.
22. Huang F, Sheng XX and Zhang HJ: DUSP26 regulates podocyte oxidative stress and fibrosis in a mouse model with diabetic nephropathy through the mediation of ROS. Biochem Biophys Res Commun 515: 410-416, 2019.
23. Guo H, Jian Z, Liu H, Cui H, Deng H, Fang J, Zuo Z, Wang X, Zhao L, Geng Y, *et al*: TGF-β1-induced EMT activation via both Smad-dependent and MAPK signaling pathways in Cu-induced pulmonary fibrosis. Toxicol Appl Pharmacol 418: 115500, 2021.
24. Chuang HC and Tan TH: MAP4K family kinases and DUSP family phosphatases in T-Cell signaling and systemic lupus erythematosus. Cells 8: 1433, 2019.
25. Fang Y, Tian X, Bai S, Fan J, Hou W, Tong H and Li D: Autologous transplantation of adipose-derived mesenchymal stem cells ameliorates streptozotocin-induced diabetic nephropathy in rats by inhibiting oxidative stress, pro-inflammatory cytokines and the p38 MAPK signaling pathway. Int J Mol Med 30: 85-92, 2012.
26. Li M, Wang L, Shi DC, Foo JN, Zhong Z, Khor CC, Lanzani C, Citterio L, Salvi E, Yin PR, *et al*: Genome-Wide meta-analysis identifies three novel susceptibility loci and reveals ethnic heterogeneity of genetic susceptibility for IgA nephropathy. J Am Soc Nephrol 31: 2949-2963, 2020.
27. Chuang HC, Chen YM, Hung WT, Li JP, Chen DY, Lan JL and Tan TH: Downregulation of the phosphatase JKAP/DUSP22 in T cells as a potential new biomarker of systemic lupus erythematosus nephritis. Oncotarget 7: 57593-57605, 2016.
28. Yue J and Lopez JM: Understanding MAPK signaling pathways in apoptosis. Int J Mol Sci 21: 2346, 2020.
29. Shen Y, Teng L, Qu Y, Liu J, Zhu X, Chen S, Yang L, Huang Y, Song Q and Fu Q: Anti-proliferation and anti-inflammation effects of corilagin in rheumatoid arthritis by downregulating NF-κB and MAPK signaling pathways. J Ethnopharmacol 284: 114791, 2022.
30. Loeffler I and Wolf G: Epithelial-to-mesenchymal transition in diabetic nephropathy: Fact or fiction? Cells 4: 631-652, 2015.
31. Xu M, Wang S, Wang Y, Wu H, Frank JA, Zhang Z and Luo J: Role of p38γ MAPK in regulation of EMT and cancer stem cells. Biochim Biophys Acta Mol Basis Dis 1864: 3605-3617, 2018.
32. Wu C, Zhou XX, Li JZ, Qiang HF, Wang Y and Li G: Pretreatment of cardiac progenitor cells with bradykinin attenuates H_2O_2-induced cell apoptosis and improves cardiac function in rats by regulating autophagy. Stem Cell Res Ther 12: 437, 2021.
33. Du X, Wang X, Cui K, Chen Y, Zhang C, Yao K, Hao Y and Chen Y: Tanshinone IIA and Astragaloside IV Inhibit miR-223/JAK2/STAT1 signalling pathway to alleviate lipopolysaccharide-induced damage in nucleus pulposus cells. Dis Markers 2021: 6554480, 2021.
34. Wada J and Makino H: Inflammation and the pathogenesis of diabetic nephropathy. Clin Sci (Lond) 124: 139-152, 2013.
35. Lim AK, Nikolic-Paterson DJ, Ma FY, Ozols E, Thomas MC, Flavell RA, Davis RJ and Tesch GH: Role of MKK3-p38 MAPK signalling in the development of type 2 diabetes and renal injury in obese db/db mice. Diabetologia 52: 347-358, 2009.
36. Li A, Peng R, Sun Y, Liu H, Peng H and Zhang Z: LincRNA 1700020I14Rik alleviates cell proliferation and fibrosis in diabetic nephropathy via miR-34a-5p/Sirt1/HIF-1α signaling. Cell Death Dis 9: 461, 2018.
37. Chen P, Yuan Y, Zhang T, Xu B, Gao Q and Guan T: Pentosan polysulfate ameliorates apoptosis and inflammation by suppressing activation of the p38 MAPK pathway in high glucosetreated HK2 cells. Int J Mol Med 41: 908-914, 2018.
38. Yoon JJ, Lee HK, Kim HY, Han BH, Lee HS, Lee YJ and Kang DG: Sauchinone protects renal mesangial cell dysfunction against angiotensin II by improving renal fibrosis and inflammation. Int J Mol Sci 21: 7003, 2020.
39. Lv ZM, Wang Q, Wan Q, Lin JG, Hu MS, Liu YX and Wang R: The role of the p38 MAPK signaling pathway in high glucose-induced epithelial-mesenchymal transition of cultured human renal tubular epithelial cells. PLoS One 6: e22806, 2011.
40. Dong Q, Jie Y, Ma J, Li C, Xin T and Yang D: Renal tubular cell death and inflammation response are regulated by the MAPK-ERK-CREB signaling pathway under hypoxia-reoxygenation injury. J Recept Signal Transduct Res 39: 383-391, 2019.
41. Ju A, Cho YC, Kim BR, Park SG, Kim JH, Kim K, Lee J, Park BC and Cho S: Scaffold Role of DUSP22 in ASK1-MKK7-JNK signaling pathway. PLoS One 11: e0164259, 2016.
42. Kosanam H, Thai K, Zhang Y, Advani A, Connelly KA, Diamandis EP and Gilbert RE: Diabetes induces lysine acetylation of intermediary metabolism enzymes in the kidney. Diabetes 63: 2432-2439, 2014.